



Three-dimensional imaging and reconstruction of the whole ovary and testis: a new frontier for the reproductive scientist

Giulia Fiorentino^{1,2}, Annapaola Parrilli³, Silvia Garagna ^{1,2,*}, and Maurizio Zuccotti ^{1,2,*}

¹Laboratory of Developmental Biology, Department of Biology and Biotechnology 'Lazzaro Spallanzani', University of Pavia, 27100 Pavia, Italy ²Center for Health Technologies, University of Pavia, Pavia 27100, Italy ³Center for X-ray Analytics, Empa, Swiss Federal Laboratories for Materials Science and Technology, Dübendorf, Switzerland

* Correspondence address. Laboratory of Developmental Biology, Department of Biology and Biotechnology 'Lazzaro Spallanzani', University of Pavia, Via Ferrata, 9, 27100—Pavia, Italy. E-mail: maurizio.zuccotti@unipv.it (M.Z.)  <http://orcid.org/0000-0003-4648-0663>; Laboratory of Developmental Biology, Department of Biology and Biotechnology 'Lazzaro Spallanzani', University of Pavia, Via Ferrata, 9, 27100—Pavia, Italy. E-mail: silvia.garagna@unipv.it (S.G.)  <http://orcid.org/0000-0003-08032405>

Submitted on June 08, 2020; resubmitted on January 14, 2021; editorial decision on January 26, 2021

ABSTRACT: The 3D functional reconstruction of a whole organ or organism down to the single cell level and to the subcellular components and molecules is a major future scientific challenge. The recent convergence of advanced imaging techniques with an impressively increased computing power allowed early attempts to translate and combine 2D images and functional data to obtain *in-silico* organ 3D models. This review first describes the experimental pipeline required for organ 3D reconstruction: from the collection of 2D serial images obtained with light, confocal, light-sheet microscopy or tomography, followed by their registration, segmentation and subsequent 3D rendering. Then, we summarise the results of investigations performed so far by applying these 3D image analyses to the study of the female and male mammalian gonads. These studies highlight the importance of working towards a 3D *in-silico* model of the ovary and testis as a tool to gain insights into their biology during the phases of differentiation or adulthood, in normal or pathological conditions. Furthermore, the use of 3D imaging approaches opens to key technical improvements, ranging from image acquisition to optimisation and development of new processing tools, and unfolds novel possibilities for multidisciplinary research.

Key words: three-dimensional imaging / volume reconstruction / organ clearing / confocal microscopy / tomography / 3D histology / folliculogenesis / spermatogenesis / ovary / testis

Introduction

The 3D functional reconstruction of an entire organ or organism down to the single cell level and to the subcellular components and molecules is a major future scientific challenge. Until a few years ago, the possibility to reproduce *in-silico* a model of an organ, to map each single cell and to integrate this spatial information with functional features, such as differentiation trajectory, physiological status and gene and protein expression profiles, was a visionary but yet unachievable objective. In more recent years, the convergence of advanced imaging techniques with an impressively increased computing power allowed early attempts to translate and combine 2D images and functional data to obtain organ 3D reconstruction.

Several network initiatives shared data collections obtained on organ serial sections analysed with classical histology, immunohistochemistry or *in situ* hybridisation alongside gene or protein expression datasets from tissue disaggregates. The eMouseAtlas (www.emouseatlas.org), an extraordinary example of community resource, originated from “The Atlas of Mouse Development” (Kaufman and Kaufman, 1992), gives the opportunity, thanks to an interactive anatomy browser, to observe hundreds of anatomical, histological, immunohistochemical and *in situ* hybridisation images ranging from the I-cell embryo to the adult.

Another initiative is ‘The Human cell atlas project’ (www.human.cellatlas.org), launched in 2017 (Regev et al., 2017) and aimed at producing an interactive 3D atlas of each human cell type that could be used for predictive modelling and interrogated to gain functional

and structural information from the organ scale to the single-cell resolution. Ambitious as it is, this project still lacks reconstructed 3D models of each organ type, i.e. *in-silico* environments that incorporate the organ's anatomical structures as well as form and identity of each single cell type together with its spatial position. Comprehensibly, this step is, of the whole project, as difficult as trying to characterise the specific molecular signature of each cell.

The work done so far on the brain, which remains the most investigated organ, represents a leading example of procedures, instrumentation and technical advancements from which to derive important tips and guidelines (Bjerke et al., 2018).

On the opposite side, the 3D modelling of gonads attempted so far is still preparatory, and an aim of the present review is to increase the awareness and stimulate interest to join forces towards this objective. Our main scope is to summarise and highlight those studies that, beginning with the collection of 2D serial images of the whole gonad volume, and following with their registration, segmentation and 3D rendering, contribute to the production of a digital 3D model. Although a large number of whole-mount *in situ* hybridisation studies published during the last 20 years have improved our understanding of gonad biology, particularly during sex determination and differentiation, a limit of this procedure is the production of a single 2D picture of the whole organ/organism that cannot be further elaborated to reach a 3D model. For these reasons, these articles were not included.

Here, we will first describe the experimental pipeline that, by combining basic imaging techniques with data processing tools, is required for organ 3D reconstruction. Then, we will summarise the results obtained so far by applying these 3D image analyses to the study of female and male gonads. We performed a systematic bibliographical search, without temporal limits, using PubMed, Web of Science and Scopus search engines employing the keywords ovary, testis, folliculogenesis, oogenesis and spermatogenesis combined with three-dimensional imaging, three-dimensional rendering, three-dimensional modelling, volume reconstruction, organ clearing, confocal microscopy, light sheet microscopy, tomography, ultrasonography, magnetic resonance imaging, micro-computed tomography, synchrotron radiation computed tomography, and histology or three-dimensional histology.

A great majority of the studies found were carried out on Mammals.

Finally, we will highlight how the study of mammalian gonads using 3D imaging approaches opens up novel possibilities for multidisciplinary research.

Key tools for whole organ 3D reconstruction

A 3D reconstruction pipeline infers the geometric 3D structure of an object through four main steps, beginning with the collection of 2D serial images, their registration, segmentation and ending with 3D rendering (Fig. 1).

Image acquisition

Images are acquired either on histological serial sections or directly on the entire organ using optical or tomographic sectioning.

With histological samples, digitalisation is an additional step required to convert physical sections into a digital collection of images covering all the object volume. Digital histological slide scanners are a fast and reliable system for automatic whole-slide scanning of racks containing hundreds of slides, but with a limited magnification of between 20 to 40X (Kumar et al., 2020). Alternatively, sections may be digitalised using a light microscope equipped with a camera, motorized XYZ stage and software for image stitching (Saalfeld, 2019). This procedure, although much slower, allows the use of objectives with a higher magnification up to 100X.

Instead, whole-organ optical sectioning is performed with confocal laser scanning microscopy (CLSM) or light-sheet fluorescence microscopy (LSFM). Samples are prepared for whole-mount immunofluorescence, which includes a tissue clearing step with large-size specimens (Richardson and Lichtman, 2015, 2017). Tissue clearing methods make organs permeable to molecular markers and optically transparent by removing lipids, the main components responsible for the heterogeneous refractive index. Five different clearing approaches have been developed: solvent-based, aqueous-based, simple immersion, hyperhydration or hydrogel-embedding (Richardson and Lichtman, 2017).

Tomography is a technique that, by using several types of penetrating electromagnetic waves, produces a true 3D reconstruction of an organ, with cubic voxels and isotropic resolution. During scanning, the sample is rotated to collect 2D projections from different rotation angles. Then, these images are used to reconstruct stacks of tomographic sections across the total 3D volume.

Registration

Image registration is the process of alignment of points that are common in subsequent images to obtain a coordinated and coherent stack. This is a step crucial when 3D reconstruction is made from histological serial sections, but it is not required with confocal or tomographic images, which are immediately available for segmentation and 3D visualisation. Two types of algorithms, the rigid (Ourselin et al., 2000) or the elastic (Davatzikos, 1997) transformation, are the most commonly used and are implemented in both open source (e.g., ImageJ, National Institutes of Health: NIH) and commercial (e.g., Amira/Avizo, Thermo Fisher Scientific) software. The rigid algorithm rotates and translates images to match pixels; instead, the elastic algorithm uses a scaling factor to stretch pixels and match them perfectly to those of a reference image.

Segmentation

Segmentation (or annotation) is the process that leads to partitioning of a 2D image into multiple regions of interest (ROIs), each with a set of pixels that has a biological meaning. Segmentation can be performed using either one or a combination of five methods: with the pixel-based method, each pixel is segmented according to its grey intensity value (*thresholding* algorithm; Otsu, 1979); the edge-based method identifies and joins front pixels to form the ROI boundaries (*level-set* function; Sethian, 1999); the region-based method, instead, considers exclusively the grey levels of neighbour pixels and joins them together (*region-growing* algorithm; Adams and Bischof, 1994). The complexity of segmentation of certain biological structures, such as the ovary itself, requires either a manual approach or the use of deep learning technologies, capable of highlighting hidden patterns, unseen by the naked eye, and use them for improved structure identification (*convolutional*

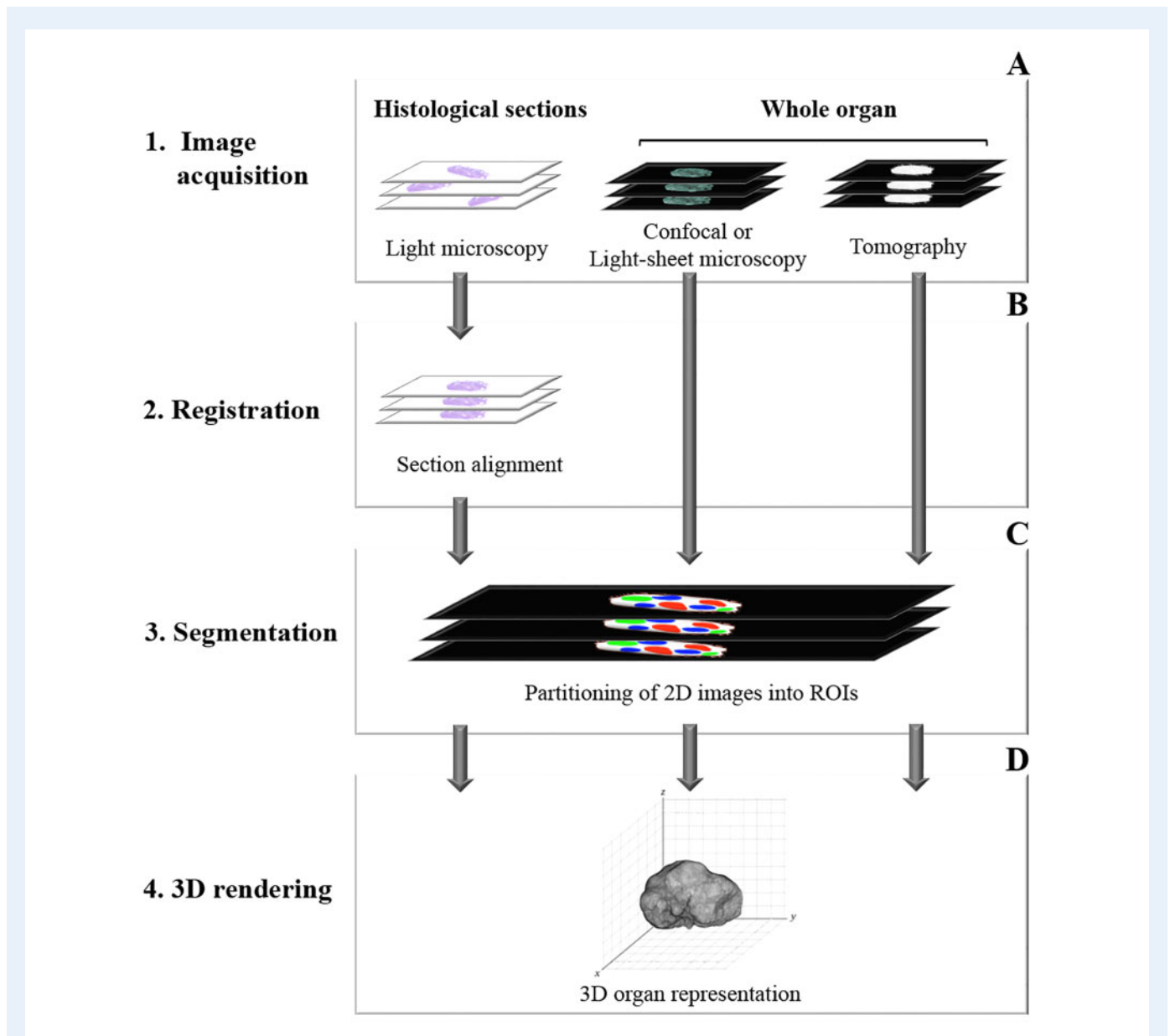


Figure 1. Four main steps of the *in-silico* organ 3D reconstruction pipeline. (A) Image acquisition is performed either from histological serial sections with light-microscopy or directly on the whole organ using optical or tomographic sectioning. (B) Registration, a required processing for the 3D reconstruction from histological sections, aligns points that are common in subsequent images to obtain a coordinated and coherent stack. (C) Segmentation is the process of partitioning each 2D image into multiple regions of interest (ROIs) with a specific biological meaning. (D) 3D rendering, the final step, gives a representation of organ 3D volume and depth by modulating light, shades and transparency.

neural network; Sahiner et al., 2019). Among the different software employed, ImageJ, ITK-SNAP (University of Pennsylvania and University of North Carolina), 3D Slicer (NIH), Imaris (Oxford Instruments), Amira/Avizo or ChimeraX (University of California San Francisco) implement segmentation algorithms.

3D rendering

3D rendering refers to Computer Graphics methods that use lightening and shading techniques to represent, on a 2D monitor, the 3D

volume and the depth of the analysed organ. Following ROI segmentation, 3D rendering of an organ is achieved using two main algorithm families: the Surface Rendering (SR) and the Volume Rendering (VR) (El Seoud and Mady, 2019). SR uses a mesh of polygons capable of approximating an isosurface from the segmented perimeter of the organ, resulting in a final object with an opaque and luminous surface. For example, the *marching cubes* is the most commonly used SR algorithm for extracting isosurfaces from a dataset. In contrast, VR shows not only the surface of an organ, but also its internal biological characteristics. VR algorithms, such as *volume ray casting*, work on voxels - 3D

counterparts of the 2D pixels - by exploiting their shading, opacity and colour features codified through RGBA values (Red, Green, Blue, Alpha, the latter specifies the opacity). 3D rendering of histological sections presents drawbacks when trying to infer tissue structures within the section thickness, as the interpolation performed to join two serial sections remains the trickiest step to solve. Among the different software employed, ImageJ, ITK-SNAP, 3D Slicer, Imaris and Amira/Avizo or ChimeraX (University of California San Francisco) implement 3D rendering algorithms.

Below is a summary of the work done using, either partially or completely, this 3D-reconstruction pipeline to study female or male gonads under normal or pathological conditions.

3D imaging and reconstruction of the mammalian ovary

The ovary is one of the most dynamic organs, not only during foetal development, when we observe its transformation from genital ridge to functional gonad, but also during adulthood when spatially

intersecting cycles of growing follicles modulate the acquisition of oocyte developmental competence. The journey of the germ cell initiates in the allantoic region of the 7.5 day *post coitum* (dpc) mouse embryo from where a group of about 100 primordial germ cells (PGCs) migrates, reaching its final destination in the genital ridges at around 10.5 dpc. Once settled, PGCs go through repeated and incomplete divisions to form cysts enclosing up to 30 interconnected germ cells (McLaren, 1984; Tam & Snow, 1981). Then, oogonia will begin to enter meiosis (12 dpc) (Wassarman, 1988) and the cysts fragment until soon after birth, when the ovary will contain only follicles enclosing single prophase I-arrested oocytes (Lei and Spradling, 2013; Pepling and Spradling, 1998, 2001). With the beginning of puberty, folliculogenesis becomes a cyclic process with the recruitment, at each cycle, of about 40 primordial follicles, a small minority of which will complete maturation and will be eventually ovulated.

Most of this information derives from studies in which the female gonads were either observed on 2D histological sections or disaggregated into separate functional units (i.e., follicles or oocytes) for further cytological and/or molecular analysis, thus altering the topographical

Table I Studies attempting a 3D reconstruction of the mammalian ovary or testis.

	Method	Instrument*	Model study	3D reconstruction pipeline step**	Reference	
Ovary	3D optical imaging	CLSM	Mouse	1	Cordeiro et al., 2015	
			Mouse	1, 3 and 4	Faire et al., 2015	
			Mouse	1 and 3	Malki et al., 2015	
			Mouse	1, 3 and 4	Feng et al., 2017	
			Mouse	1 and 3	Rinaldi et al., 2017	
		LSFM	Mouse	1, 3 and 4	Kagami et al., 2018	
			Rat	1, 3 and 4	Ma et al., 2018	
			Mouse	1, 3 and 4	Oren et al., 2018	
			Mouse	1, 3 and 4	McKey et al., 2020	
		Tomography	microCT	Rat, dog, cat, cow, horse, pig, donkey	1	Paulini et al., 2017
				Mouse	1, 3 and 4	Fiorentino et al., 2020
			MRI	Mouse	1 and 3	Hensley et al., 2007
			Ultrasonography	Mouse	1	Mircea et al., 2009
3D histology	Synchrotron Radiation CT	Human	1, 3 and 4	Nylander et al., 2017		
		Mouse	1, 3 and 4	Kim et al., 2012		
	Light microscopy	Horse	1 - 4	Kimura et al., 2005		
		Cat	1 - 4	Prozorowska et al., 2018		
		Human	1, 3 and 4	Combes et al., 2009		
Testis	3D optical imaging	CLSM	Mouse	1, 3 and 4	Malki et al., 2015	
			Mouse	1 and 3	Kaufman et al., 2020	
			Mouse	1, 3 and 4	Nguyen et al., 2020	
			Mouse	1, 3 and 4	Belle et al., 2017	
			Human	1, 3 and 4	Silva et al., 2015	
		Tomography	microCT	Mouse	1, 3 and 4	Thet-Thet-Lwin et al., 2018
			Synchrotron	Rat	1, 3 and 4	
			X-ray imaging			
		3D histology	Light microscopy	Mouse	1 - 4	Nakata et al., 2015
				Mouse	1 - 4	Nakata et al., 2017

*: CLSM, confocal laser scanning microscopy; LSFM, light-sheet fluorescence microscopy; microCT, micro-computed tomography.

** : 1, acquisition; 2, registration; 3, segmentation; 4, 3D rendering.

representation of events occurring during oogenesis. Recent improvements in imaging techniques give powerful insights to extend our comprehension of follicle growth and its relationship with the surrounding vasculature (Feng et al., 2018).

During the past 5 years, using 3D optical imaging, tomography or 3D histology techniques, a total of 18 papers attempted a 3D representation of the whole mammalian ovary at different developmental and postnatal stages (Table 1). Among these, eight studies completed all four steps of the reconstruction pipeline, from image acquisition, registration (when needed), segmentation and rendering, up to the proposal of a 3D model of the ovary. Thanks to these experiments, several aspects of oocyte and follicle maturation, vessel formation and remodelling were revisited or studied for the first time in the 3D context of the normal or pathological ovary, throughout foetal and adult oogenesis and folliculogenesis.

3D optical imaging

In one of the earliest studies of this kind, Cordeiro et al. (2015), working on confocal image stacks of whole-mount ovaries (pipeline step 1; Fig. 1), challenged the production line hypothesis (Henderson and Edwards, 1968) according to which the first oogonia entering meiosis (12.5 dpc) and undertaking prophase I arrest, will also be those oocytes recruited for the first wave of folliculogenesis at the beginning of puberty. By using transgenic mice for *Mvh*, *Gdf9* and *Zp3* promoters—whose proteins mark simultaneously germ cells, primordial or growing follicles, respectively—the 3D approach used allowed the drawing of a geographic map of the early stages of follicle formation, from 12.5 dpc to 12 days post-birth (dpb). These results highlighted the presence of two different spatial localisations for the group of oogonia that first enter meiosis (12.5 dpc, anterior-ventral region of the ovary) and for those oocytes that are recruited at the first wave of follicles growth (3–4 dpb, anterior-dorsal region of the ovary). Finally, these data suggested a key role of both cortex and medulla differentiation in recruitment of the first follicles.

Another group of studies employed 3D confocal analysis of the whole ovary (pipeline step 1) to obtain a more accurate oocyte count compared to that obtained with traditional histology. Malki and collaborators studied the mouse ovary during a developmental window between 15.5 and 18.5 dpc, when foetal oocyte attrition occurs (Malki et al., 2015). Using the hyperhydration clearing procedure ScaleA2, together with the Tra98 germ cell-specific marker, they described a significantly lower oocytes loss (27%) compared to that previously determined using 2D histological serial sections (44%). In addition, the authors proposed a 3D rendering (pipeline step 4) of the volume occupied by germ cells in 18.5 dpc ovary.

Similarly, using the ScaleS4(0) hyperhydration clearing procedure and nuclear (p63) and cytoplasmic (mouse vasa homolog: MVH) oocyte-specific markers on 5-day-old mouse ovaries, Rinaldi et al. (2017) evaluated the potential of pharmacological inhibition of kinase 2 (CHK2), a key element of the oocyte DNA damage checkpoint response, to preserve ovarian function during radiotherapeutic treatment. Oocyte count, performed with the Analyze particle function of Fiji-ImageJ software on 3D projections of confocal planes, showed that CHK2 inactivation preserved oocytes and their viability.

Another study aimed at identifying the 3D spatial localisation and counting of primordial follicles in day 1 to 24-week-old mice. Confocal

images of whole-mount ovaries were immuno-stained with the primordial oocyte-specific Nobox marker (Faire et al., 2015) and analysed with Velocity 6.2 (Improvision) image processing tool and a custom-made Matlab program. This work showed—with improved accuracy compared to 2D histological counts (Gosden et al., 1983; Richardson et al., 1987) - that the reserve of primordial follicles plays a key role in fertility maintenance, and that a drop in primordial follicle number correlates with ovulation arrest. In addition, the counting of small non-growing primordial follicles in day 1 to 24-week-old ovaries was used to build a linear model that predicted a decreased number during adulthood, down to about 500 primordial follicles at the end of reproductive life (Faire et al., 2015).

This age-dependent follicle loss has been substantiated by a further 3D optical image study. The use of another tissue clearing method, CLARITY, combined with advanced image processing tools (Imaris), led to an important contribution to the 3D reconstruction of the mouse ovary together with its vasculature (Feng et al., 2017) (pipeline steps 1, 3 and 4). This study described and produced *in-silico* models of the spatial relationship between follicles during mouse life, from birth to senescence, and the role of ovarian blood vessel remodelling throughout folliculogenesis. Specifically, the use of immuno-markers for primordial, growing or fully-grown antral follicles allowed information to be obtained on several key aspects of the folliculogenetic process in a 3D context. For example, the count and spatial localisation of the different follicle types confirmed an age-dependent loss (Faire et al., 2015). Furthermore, the use of platelet endothelial cell adhesion molecule-1, an endothelial cell marker, allowed the modelling of a follicle-vasculature spatial interaction map, which showed that: follicles are not randomly distributed inside the organ volume, but are located along main vasculature branches; after FSH-mediated follicle recruitment, the avascular primordial follicles start growing and secrete vascular endothelial growth factor A (VEGFA) to promote neo-angiogenesis; and in VEGFA mutant mice or mice treated with axitinib, a VEGF receptor-targeted tyrosine kinase inhibitor, vasculature remodelling is arrested causing defective ovulation.

Whilst the studies described above made use of classical CLSM, four recent papers combined LSFM with clearing procedures (Kagami et al., 2018; Ma et al., 2018; Oren et al., 2018; McKey et al., 2020). Although a drawback of LSFM is its lower magnification power and resolution, the laser shaped into a light sheet orthogonal to the sample allows a larger field of view and faster acquisition of intact organs or entire small animals with minimal sample exposure and photobleaching (Santi, 2011).

The combination of LSFM with WOBLI (whole-organ blood and lymphatic vessels imaging), a new clearing method developed for ovary, uterus, lung and liver, allowed an important step forward for 3D imaging of blood and lymphatic vessels, extensively involved in remodelling and neo-angiogenesis during adult folliculogenesis (pipeline steps 1, 3 and 4; Oren et al., 2018). This method identified and spatially localised even the smallest capillaries surrounding growing follicles, and, when combined with processing tools implemented in ImageJ and Imaris, performed a quantitative analysis of the 3D vascular network, thereby extracting preliminary data of vessel size in terms of diameter (mean: 14 μ m), total organ vasculature length (mean: 1.38 cm), and vasculature length surrounding single antral follicles (mean: 45.40 mm).

Another study, combining LSFM with the clearing procedure CUBIC on ovaries of EGFP transgenic mice, described the 3D localisation of

individual follicles and of their oocyte, granulosa and theca cell components (pipeline steps 1, 3 and 4; Kagami et al., 2018).

The use of CUBIC together with the clearing method iDISCO and the immunostaining for smooth muscle actin alpha (α SMA; interstitial marker), anti-Müllerian hormone (AMH; granulosa cells), and MVH (oocyte) allowed the identification of all follicle types within the adult mouse ovary (McKey et al., 2020). Images, acquired through either LSFM or CLSM, were further processed with Imaris software obtaining automatic segmentation and 3D rendering of individual follicles (pipeline steps 1, 3 and 4). In addition, labelling of the whole ovary with ENDOMUCIN for endothelial cells and with TUJ1 for nerves permitted the observation of the ovarian main vasculature and microcapillaries, and of the intricate network of neural projections that extend from the medulla towards the cortex.

LSFM and CLARITY were also applied to study ovarian pathologies, such as polycystic ovary syndrome (PCOS), which causes disruption of the oestrus cycle and anovulation (pipeline steps 1, 3 and 4; Ma et al., 2018). Using tyrosine hydroxylase to identify different follicles morphologically, a recent study showed a decrease of antral and a lack of fully-grown preovulatory follicles in 5α -dihydrotestosterone-induced PCOS-like rat ovaries. They further used PECAMI and proliferating cell nuclear antigen to mark ovarian vasculature and neo-vascularity, respectively, suggesting that problems in follicle maturation and anovulation in women with PCOS might relate to atypical organisation of the ovarian vasculature around antral follicles, with changes in size and number of local blood vessels and impaired neo-angiogenesis.

Tomography

Tomography is, of all the imaging methods, the only one that gives a true 3D model with cubic voxels and isotropic resolution. There are four main tomographic techniques used to study the ovary *in vivo* or *ex vivo*: MRI (Van Reeth et al., 2012), ultrasonography (US; Campbell, 2019), synchrotron radiation computed tomography (SR-CT; Zehbe et al., 2010) and micro-computed tomography (microCT; Rawson et al., 2020). The results obtained so far with MRI and US are limited to the identification of large corpora lutea, pre-ovulatory and antral follicles. Only the use of SR-CT or microCT allowed the localisation of small pre-antral follicles.

Using a transgenic mouse model of ovarian cancer, MRI was used for volume quantification (pipeline steps 1 and 3) of epithelial ovarian cancer progression *in vivo* (Hensley et al., 2007).

The efficacy of a tomographic approach as a diagnostic tool for PCOS was highlighted by comparing traditional 2D trans-vaginal ultrasonography (TVUS) with 3D TVUS to measure human ovarian volume and estimate antral follicles number (Nylander et al., 2017). A limit of the 2D approach is its approximation to an ovoid ovary shape and, therefore, an underestimation of its volume and follicle number. Instead, 3D TVUS, combined with segmentation (VOCAL) and volume (SonoAVC) analysis tools, allowed a 3D reconstruction (pipeline steps 1, 3 and 4) and a more precise estimation of the ovary shape and volume, together with an accurate counting of antral follicles. In addition, TVUS-mediated antral follicle count, turned out to be efficient in predicting the number of oocytes retrieved in IVF cycles after FSH stimulation.

Trans-abdominal ultrasonography combined with intravital multiphoton microscopy was used to study the role of vasoconstriction

occurring at the time of mouse follicle rupture (Migone et al., 2016). This study used intravital multiphoton microscopy to analyse, during ovulation, the diameter and the blood flow of small vessels and the thickness of the apical pre-ovulatory follicle wall (pipeline step 1). Comparing wild-type with mice deficient for vascular smooth muscle surrounding theca vessels (Amhr2cre/+SmoM2), they showed a direct correlation between the presence/absence of vasoconstriction and follicle rupture/block of ovulation. Using trans-abdominal ultrasonography *in vivo* allowed an increase in the imaging depth through the entire pre-ovulatory follicle. Altogether, these results demonstrated that vasoconstriction and decreased blood flow are restricted to the external apex of pre-ovulatory follicles, highlighting their key role in ovulation.

Another ultrasound technique used for *in vivo* analysis of the adult mouse ovary, although only in a single study, is ultrasound biomicroscopy (UBM), a near-microscopic resolution tomography (Mircea et al., 2009). Comparison with digitalised histological sections showed the reliability of the UBM technique for the counting of corpora lutea, and antral and pre-ovulatory follicles > 300 μ m in diameter (pipeline step 1).

SR-CT was used, for the first time, on intact ovaries of vaccinia-related kinase 1 (VRK1)-deficient mice, to investigate the role of VRK1 in modulating cell cycle progression during oogenesis (Kim et al., 2012). This 3D analysis allowed an accurate reconstruction and quantification (pipeline steps 1,3 and 4) of follicles from the pre-antral to the pre-ovulatory stage. Compared to wild-type, the number of pre-antral and antral follicles in VRK1-deficient ovaries was significantly reduced by 38% and 46%, respectively. Furthermore, the volume of VRK1-deficient antral and fully-grown pre-ovulatory oocytes decreased by 42% and 37%, respectively, suggesting a reduced quality.

To date, two studies have attempted the characterisation of the ovarian organisation using microCT. In the first, Paulini et al. (2017) analysed seven different fixed mammalian ovaries: rat, dog, cat, cow, horse, pig and donkey. Using iodine tincture as the contrast agent, this X-ray imaging technique led to the distinction between cortex and medulla regions, and the identification of corpora lutea and antral follicles (pipeline step 1). In addition, microCT images allowed the visualisation of the main blood vessels and their distribution.

In a more recent study (Fiorentino et al., 2020), 1.5 μ m/pixel microCT imaging of the adult mouse ovary, combined with ImageJ and Avizo image processing tools, allowed the identification, 3D mapping and counting of secondary to fully-grown antral follicles and corpora lutea (pipeline steps 1, 3 and 4). This analysis demonstrated that all follicle types are equally distributed between the dorsal and ventral regions of the ovary, and that each ovarian sector contains an equal number of the different follicle types. For the first time, microCT analysis brought up the main functional components of the growing follicle, such as the granulosa and cumulus cells, the zona pellucida and the oocyte with its nucleus. Furthermore, it allowed the visualisation and 3D modelling of the main ovarian vasculature, from the largest (150 μ m in diameter) to the small (35 μ m) vessels present in the medulla region.

3D histology

3D histology emerges as an alternative that could offer a number of important advantages with regard to sub-cellular resolution and the possibility to use a large portfolio of staining procedures, specific for different cell organelles and physiological activities. The efforts made

over recent years in developing this technique may be highlighted, for example, by its immediate impact in improving disease diagnosis (Griffin and Treanor, 2017).

To date, only two studies have employed 3D histology (pipeline steps 1-4) for the analysis of the ovary. A study analysed the development of the cat urogenital system during the prenatal period and in the adult, describing changes in size and position of the ovary within the body (Prozorowska et al., 2018). The other showed, in the horse, the spatial localisation of growing follicles in the cortical region, and of the corpus luteum near to the ovulation fossa, a specific region where ovulation occurs (Kimura et al., 2005).

3D imaging and reconstruction of the mammalian testis

The main compartments of the male adult gonad are the interstitial region, the seminiferous tubules and the rete testis that converges into the epididymis outside the testis. The tubules encapsulate the seminiferous epithelium from which differentiated spermatozoa will originate.

As for the female, the history of the male germ cell initiates in the foetus. Upon gonad differentiation (12.5 dpc in the mouse) the sex cords will form the seminiferous tubules enclosing spermatogonia and Sertoli cells, the only two cell types that will populate the seminiferous epithelium throughout development and until puberty. After birth, mouse spermatogonia type As undergo multiplying mitotic divisions to form spermatogonia type A1, followed by A2, A3, A4, Intermediate and type B. At puberty, type B spermatogonia enter meiosis, thus building up a multi-stratified seminiferous epithelium made of differentiating layers of primary and secondary spermatocytes, round and elongating spermatids: the latter are released, as mature sperm, into the tubule lumen, to be transported towards the rete testis first, and then into the epididymis where they will be stored until ejaculation. Male germ cell differentiation, from spermatogonia on the basal membrane to spermatozoa in the lumen, is described through a number of stages of the cycle of the seminiferous epithelium (e.g., 12 in the mouse or six in human), defined as associations of specific types of spermatogonia, spermatocytes, round and elongated spermatids (Oakberg, 1956).

During the past 5 years, eight studies have attempted 3D imaging and reconstruction of the whole mammalian testis using 3D optical imaging, tomography or 3D histology. These studies allowed the 3D description of the seminiferous tubules' organisation and localisation inside the testis and contributed insights into the progression of the cycle of the seminiferous epithelium, in normal or pathological conditions.

3D optical imaging

In a very recent study, whole-mount immunofluorescence on intact E12.5-14.5 foetal mouse testes was used to investigate the apoptotic events occurring at the time when PGCs initiate differentiation to pro-spermatogonia (Nguyen et al., 2020; pipeline step 1, 3 and 4). Immuno-staining with Tra98 and the late-stage apoptotic marker cleaved-PARP showed an increasing number of apoptotic PGCs from E12.5 to E14.5; these dying cells were clustered and evenly distributed inside the gonad. Interestingly, the frequency of apoptotic PGCs in *Tex14^{-/-}* testes lacking intercellular bridges did not differ from that of

wild-type gonads; also, PGCs displayed a clustered distribution, suggesting that the apoptotic potential is maintained in disconnected germ cells. An integration of these results with single-cell RNA-sequencing analyses allowed the identification of an apoptosis-susceptible PGCs subpopulation isolated from E13.5 testes. These PGCs exhibited a higher DNA methylation profile that correlated with impaired expression of genes involved in cell differentiation.

In an elegant study, whole-mount mouse 12.5 to 15.5 dpc male gonads were immuno-labeled with the Sertoli cell marker SOX9, the vascular marker VE-cadherin, and counterstained with anti-mouse Alexa 555, to demonstrate that testis cords arise through a strong 3D remodelling of a primitive cord network (pipeline steps 1, 3 and 4; Combes et al., 2009). Specifically, 3D models, reconstructed using the program IMOD (University of Colorado), highlighted that cords: are present in a number higher than previously reported; initially form a network of irregular clusters of Sertoli and germ cells, subsequently remodelled to form more regular parallel loops; remodel differently in mesonephric and coelomic organ domains and their specification is not stereotypic. Focusing always on the foetal male gonad, Malki et al. (2015) applied the whole-mount approach developed for the ovary (see above) to identify and count the presence of ~14400 germ cells in E15.5 mouse testis.

Kaufman et al. (2020) combined a clearing procedure with immuno-staining and confocal imaging for the 3D study of ~ 3 mm³ blocks of adult mouse testes. The use of ubiquitin C-terminal hydrolase (UCH-L1) allowed the staining of spermatogonia and Sertoli cells, while SMA, a marker for smooth muscle actin, labelled peritubular myoid cells and muscular layers of blood vessels, simultaneously identifying cells located both in seminiferous tubules and in interstitial tissue. The volume reconstruction, obtained as a 3D projection of serial confocal images (pipeline steps 1, 3 and 4), permitted the spatial characterisation of seminiferous tubules with near-histological resolution and subcellular details, and also showed the physical relationship between tubules and interstitial surrounding vasculature.

In a further study, by combining the 3DISCO clearing method with LSFM, Belle et al. (2017) investigated the urogenital system during the first trimester of human development, when sex determination occurs. By using a double immuno-staining for Pax2 (Müllerian and Wolffian duct cells) and Plvap (endothelial cells), the authors demonstrated a correlation between the avascularisation of the male Müllerian duct and its regression at gestational week 10 (pipeline steps 1, 3 and 4).

Tomography

To date, a single study identified the seminiferous tubules 3D organization using microCT (Silva et al., 2015). In this article, testes underwent dehydration and staining with an alcohol-based iodine contrast agent in order to obtain a homogeneous diffusion and limit organ shrinkage during imaging. The use of this method on the adult mouse testis allowed also the identification of the tunica albuginea and a 3D rendering of the organ surface, including the epididymis (pipeline steps 1, 3 and 4).

In addition, SR-CT, with 26 µm/pixel resolution, was used *ex vivo* to study testicular seminomas in aged rats (Thet-Thet-Lwin et al., 2018), observing not only a heterogeneous organisation inside the tumour mass, but also the presence of a rich vasculature involved in tumour growth (pipeline 1,3 and 4).

3D histology

The most insightful of all studies that attempted a male gonad 3D reconstruction from histological sections is that of [Nakata et al. \(2015\)](#). These authors determined the number, length and 3D spatial relationship among seminiferous tubules from a collection of hematoxylin and eosin stained serial sections of a mouse adult testis. A total of 11 seminiferous tubules, each ~140 mm in length, were individually identified, manually segmented, reconstructed and superimposed on the 3D volume of the

testis to observe their spatial localisation (pipeline steps 1-4). The 3D model revealed that tubules are stacked in regular layers, most presenting a funnel shape with both ends connected to the rete testis.

Following periodic acid-Schiff-hematoxylin staining of testis serial sections of newborn, 21-day-old and adult mice, and using the acrosome size and shape as staging markers, the authors identified, inside each single tubule, the interval sequence of I-VI, VII-VIII and IX-XII stages of the cycle of the seminiferous epithelium ([Nakata et al., 2017](#)), and

	Method	Pros	Cons
A	3D optical imaging	Molecular markers allow the identification of follicles from primordial to preovulatory, and of the main vasculature	Lack of an isotropic resolution along the x, y, z axes
B	Tomography (SR-CT)	Isotropic resolution along the x, y, z axes allows a true 3D reconstruction	Impossible to use molecular markers; limited resolution does not allow the identification of primordial to secondary follicles
C	Tomography (microCT)	Isotropic resolution along the x, y, z axes allows a true 3D reconstruction; localisation of secondary to preovulatory follicles, with their internal components, and of the main vasculature	Impossible to use molecular markers; limited resolution does not allow the identification of primordial and primary follicles
D	3D histology	Specific histological staining allows 3D reconstruction of the seminiferous tubules and the identification of the main seminiferous epithelium stages	Physical sectioning of the whole testis; lack of an isotropic resolution along the x, y, z axes

Figure 2. In-silico 3D models of mouse ovary and testis obtained with 3D optical imaging, tomography or 3D histology. For each method used, the main advantages and disadvantages are listed. The illustrations are taken from the publications listed below and modified under the terms of the Creative Commons Attribution License (CC BY). **(A)** Combination of [Fig. 1A](#) and [Fig. 5A](#) from [Feng et al. \(2017\)](#). Upper panel: identification and counting of follicles (green and red) and corpora lutea (CL: yellow) during female ageing; lower panel: main ovarian vasculature. **(B)** Modification of [Fig. 1](#) from [Kim et al. \(2012\)](#). i) 3D rendering of the whole adult ovary. Navy, pre-antral follicle; green, antral follicle; violet, Graffian follicle; yellow, corpus luteum. ii and iii) 3D rendering of an antral and a Graffian follicle, respectively. Yellow arrow, antrum cavity; red arrow, oocyte. **(C)** Combination of [Figs 3B and 2E](#) from [Fiorentino et al. \(2020\)](#). i) Volume rendering of the different type of follicle present in the adult ovary (Pedersen and Peters, 1968) from the preantral secondary (T4) to the fully-grown antral (T8) follicle. Blue, T4; red, T5; pink, T6; green, T7; orange, T8; yellow, corpus luteum. ii) Combined 3D rendering of microCT sections of the ovary and of the main vasculature. **(D)** Modification of [Fig. 2](#) from [Nakata et al. \(2015\)](#). Reconstruction of the 11 seminiferous tubules present in an adult testis, each represented with a specific colour. Pink, rete testis. A further identification of the seminiferous epithelium stages was described by [Nakata et al. \(2017\)](#).

demonstrated that the first spermatogenic wave occurs preferentially near to the rete testis. Also, the reconstructed 3D model showed a regular testis architecture maintained from birth to adulthood (pipeline steps 1-4).

Conclusion and future perspectives

Although the number of studies conducted is still small, the results obtained so far already show the importance of working towards a 3D modelling of the gonads and highlight how this perspective will improve our knowledge on several key features of their biology during differentiation or adulthood, in normal or pathological conditions. [Figure 2](#) summarises the main results of those studies that, by completing the four stages of the reconstruction pipeline, proposed a 3D *in silico* model of the gonad.

Overall, the data on the ovary highlighted crucial aspects of the temporal, spatial and quantitative dynamics of the oogenetic process, from the entry of oogonia into meiosis (foetus) to the first recruitment of follicles (puberty) and their subsequent maturation (adult). Furthermore, they described the timing of its organisation into a medulla and a cortex region, and the 3D relationship between growing follicles and their surrounding capillaries.

Likewise, testis 3D modelling disclosed a specific internal spatial organisation of the seminiferous tubules, which appeared arranged into regular layers, with both ends directly linked to the rete testis. Importantly, the region of connection between rete testis and tubules also corresponds to the site where the earliest spermatogenic waves occur.

As a future perspective, the integration of a 3D reconstructed model with specific molecular information obtained by directly mapping RNAs or proteins inside the tissue will contribute to the production of a 3D functional atlas of the studied organ. Examples of recent technologies that allow the acquisition of this information at a high multiplexed level are: matrix-assisted laser desorption/ionization mass spectrometry imaging (MALDI MSI), which detects *in situ* the peptide or lipid content on histological sections and allows a 3D mapping of their localisation ([Neagu, 2019](#)); multiparameter ion beam imaging (MIBI), a spectrometry that detects antibodies tagged with metal reporters ([Angelo et al., 2014](#)); spatial transcriptomics, that identifies and maps genes activity directly on tissue sections ([VanHorn and Morris, 2020](#)); quantitative hybridisation chain reaction (qHCR) imaging quantifies mRNAs in the anatomical context of whole-mount samples ([Choi et al., 2018](#)); digital hybridisation chain reaction (dHCR) imaging gives mRNA quantification *via* single-molecule imaging in thick auto-fluorescent samples ([Choi et al., 2018](#)). Also, combined with tissue clearing or tissue expansion, other recent technologies include multiplexed error robust FISH (MERFISH), that can simultaneously analyse thousands of cells of a tissue ([Chen et al., 2015](#)), and seq-FISH that can image hundreds of RNAs in single-cells ([Lubeck et al., 2014](#)).

Altogether, these studies serve as examples that unfold the potential of a 3D approach to gain insights into the biology of the ovary and testis, and, also, to propose key technical novelties along all steps of the reconstruction process, from image acquisition to the optimisation and

development of new image processing tools and quantitative computational models.

Data availability

No new data were generated or analysed in support of this research.

Acknowledgments

The authors thank Merck-MilliQ Laboratory Water Solutions for support.

Authors' roles

Conception and design: G.F., A.P., S.G., M.Z.; literature search: G.F., M.Z.; manuscript writing: G.F., S.G., M.Z.

Funding

This work was made possible thanks to support from the Italian Ministry of Education, University and Research (MIUR) Dipartimenti di Eccellenza Program (2018–2022) to the Department of Biology and Biotechnology 'L. Spallanzani', University of Pavia, and a grant from the University of Pavia (FRG 2018).

Conflict of interest

The authors have no conflict of interest to declare.

References

- Adams R, Bischof L. Seeded region growing. *IEEE Trans Pattern Anal Machine Intell* 1994;**16**:641–647.
- Angelo M, Bendall SC, Finck R, Hale MB, Hitzman C, Borowsky AD, Levenson RM, Lowe JB, Liu SD, Zhao S, Natkunam Y et al. Multiplexed ion beam imaging of human breast tumors. *Nat Med* 2014;**20**:436–442.
- Belle M, Godefroy D, Couly G, Malone SA, Collier F, Giacobini P, Chédotal A. Tridimensional Visualization and Analysis of Early Human Development. *Cell* 2017;**169**:161–173.e12.
- Bjerke IE, Øvsthus M, Papp EA, Yates SC, Silvestri L, Fiorilli J, Pennartz C, Pavone FS, Puchades MA, Leergaard TB et al. Data integration through brain atlasing: Human Brain Project tools and strategies. *Eur Psychiatr* 2018;**50**:70–76.
- Campbell S. Ultrasound Evaluation in Female Infertility: Part I, the Ovary and the Follicle. *Obstet Gynecol Clin North Am* 2019;**46**: 683–696.
- Chen KH, Boettiger AN, Moffitt JR, Wang S, Zhuang X. RNA imaging. Spatially resolved, highly multiplexed RNA profiling in single cells. *Science* 2015;**348**:aaa6090–aaa6090.
- Choi HMT, Schwarzkopf M, Fornace ME, Acharya A, Artavanis G, Stegmaier J, Cunha A, Pierce NA. Third-generation *in situ* hybridization chain reaction: multiplexed, quantitative, sensitive, versatile, robust. *Development* 2018;**145**:dev165753.

- Combes AN, Lesieur E, Harley VR, Sinclair AH, Little MH, Wilhelm D, Koopman P. Three-dimensional visualization of testis cord morphogenesis, a novel tubulogenic mechanism in development. *Dev Dyn* 2009;**238**:1033–1041.
- Cordeiro MH, Kim SY, Ebbert K, Duncan FE, Ramalho-Santos J, Woodruff TK. Geography of follicle formation in the embryonic mouse ovary impacts activation pattern during the first wave of folliculogenesis. *Biol Reprod* 2015;**93**:88–1.
- Davatzikos C. Spatial transformation and registration of brain images using elastically deformable models. *Comput Vis Image Underst* 1997;**66**:207–222.
- El Seoud MSA, Mady AS. A Comprehensive Review on Volume Rendering Techniques. In: Proceedings of the 2019 8th International Conference on Software and Information Engineering, Egypt, Cairo. 2019; pp. 126–131.
- Feng Y, Cui P, Lu X, Hsueh B, Billig FM, Yanez LZ, Tomer R, Boerboom D, Carmeliet P, Deisseroth K et al. CLARITY reveals dynamics of ovarian follicular architecture and vasculature in three-dimensions. *Sci Rep* 2017;**7**:1–13.
- Faire M, Skillern A, Arora R, Nguyen DH, Wang J, Chamberlain C, German SM, Fung JC, Laird DJ. Follicle dynamics and global organization in the intact mouse ovary. *Dev Biol* 2015;**403**:69–79.
- Feng Y, Tamadon A, Hsueh AJW. Imaging the ovary. *Reprod Biomed Online* 2018;**36**:584–593.
- Fiorentino G, Parrilli A, Garagna S, Zuccotti M. Three-Dimensional Micro-Computed Tomography of the Adult Mouse Ovary. *Front Cell Dev Biol* 2020;**8**.
- Gosden RG, Laing SC, Felicio LS, Nelson JF, Finch CE. Imminent oocyte exhaustion and reduced follicular recruitment mark the transition to acyclicity in aging C57BL/6j mice. *Biol Reprod* 1983;**28**:255–260.
- Griffin J, Treanor D. Digital pathology in clinical use: where are we now and what is holding us back? *Histopathology* 2017;**70**:134–145.
- Henderson SA, Edwards RG. Chiasma frequency and maternal age in mammals. *Nature* 1968;**218**:22–28.
- Hensley H, Quinn BA, Wolf RL, Litwin SL, Mabuchi S, Williams SJ, Williams C, Hamilton TC, Connolly DC. Magnetic resonance imaging for detection and determination of tumor volume in a genetically engineered mouse model of ovarian cancer. *Cancer Biol Ther* 2007;**6**:1717–1725.
- Kagami K, Shinmyo Y, Ono M, Kawasaki H, Fujiwara H. Three-dimensional evaluation of murine ovarian follicles using a modified CUBIC tissue clearing method. *Reprod Biol Endocrinol* 2018;**16**:72.
- Kaufman MH, Kaufman MH. *The Atlas of Mouse Development*. London, UK: Academic press, 1992.
- Kaufman JA, Castro MJ, Ruiz SA, Jentarra GM, Chavira B, Rodriguez-Sosa JR. Clearing, immunofluorescence, and confocal microscopy for the three-dimensional imaging of murine testes and study of testis biology. *J Struct Biol* 2020;**209**:107449.
- Kim J, Choi YH, Chang S, Kim KT, Je JH. Defective folliculogenesis in female mice lacking Vaccinia-related kinase 1. *Sci Rep* 2012;**2**:1–7.
- Kimura J, Hirano Y, Takemoto S, Nambo Y, Ishinazaka T, Himeno R, Mishima T, Tsumagari T, Yokota H. Three-dimensional Reconstruction of the Equine Ovary. *Anatom Histol Embryol* 2005;**34**:48–51.
- Kumar N, Gupta R, Gupta S. Whole Slide Imaging (WSI) in Pathology: Current Perspectives and Future Directions. *J Digit Imaging* 2020;**33**:1034–1040.
- Lei L, Spradling AC. Female mice lack adult germ-line stem cells but sustain oogenesis using stable primordial follicles. *PNAS* 2013;**110**:8585–8590.
- Lubeck E, Coskun AF, Zhiyentayev T, Ahmad M, Cai L. Single-cell in situ RNA profiling by sequential hybridization. *Nat Methods* 2014;**11**:360–361.
- Ma T, Cui P, Tong X, Hu W, Shao LR, Zhang F, Li X, Feng Y. Endogenous Ovarian Angiogenesis in Polycystic Ovary Syndrome-Like Rats Induced by Low-Frequency Electro-Acupuncture: The CLARITY Three-Dimensional Approach. *IJMS* 2018;**19**:3500.
- Malki S, Tharp ME, Bortvin A. A whole-mount approach for accurate quantitative and spatial assessment of fetal oocyte dynamics in mice. *Biol Reprod* 2015;**93**:113–1.
- McKey J, Cameron LA, Lewis D, Batchvarov IS, Capel B. Combined iDISCO and CUBIC tissue clearing and lightsheet microscopy for in toto analysis of the adult mouse ovary. *Biol Reprod* 2020;**102**:1080–1089.
- McLaren A. Meiosis and differentiation of mouse germ cells. *Symp Soc Exp Biol* 1984;**38**:7–23.
- Migone FF, Cowan RG, Williams RM, Gorse KJ, Zipfel WR, Quirk SM. In vivo imaging reveals an essential role of vasoconstriction in rupture of the ovarian follicle at ovulation. *Proc Natl Acad Sci USA* 2016;**113**:2294–2299.
- Mircea CN, Lujan ME, Jaiswal RS, Singh J, Adams GP, Pierson RA. Ovarian imaging in the mouse using ultrasound biomicroscopy (UBM): a validation study. *Reprod Fertil Dev* 2009;**21**:579–586.
- Nakata H, Wakayama T, Sonomura T, Honma S, Hatta T, Iseki S. Three-dimensional structure of seminiferous tubules in the adult mouse. *J Anat* 2015;**227**:686–694.
- Nakata H, Sonomura T, Iseki S. Three-dimensional analysis of seminiferous tubules and spermatogenic waves in mice. *Reproduction* 2017;**154**:569–579.
- Neagu AN. Proteome Imaging: From Classic to Modern Mass Spectrometry-Based Molecular Histology. *Adv Exp Med Biol* 2019;**1140**:55–98.
- Nguyen DH, Soygur B, Peng SP, Malki S, Hu G, Laird DJ. Apoptosis in the fetal testis eliminates developmentally defective germ cell clones. *Nat Cell Biol* 2020;**22**:1423–1435.
- Nylander M, Frøssing S, Bjerre AH, Chabanova E, Clausen HV, Faber J, Skouby SO. Ovarian morphology in polycystic ovary syndrome: estimates from 2D and 3D ultrasound and magnetic resonance imaging and their correlation to anti-Müllerian hormone. *Acta Radiol* 2017;**58**:997–1004.
- Oakberg EF. A description of spermiogenesis in the mouse and its use in analysis of the cycle of the seminiferous epithelium and germ cell renewal. *Am J Anat* 1956;**99**:391–413.
- Oren R, Fellus-Alyagor L, Addadi Y, Bochner F, Gutman H, Blumenreich S, Dafni H, Dekel N, Neeman M, Lazar S. Whole Organ Blood and Lymphatic Vessels Imaging (WOBLI). *Sci Rep* 2018;**8**:1–9.
- Otsu N. A threshold selection method from gray-level histograms. *IEEE Trans Syst, Man, Cybern* 1979;**9**:62–66.

- Ourselin S, Roche A, Prima S, Ayache N. *International Conference on Medical Image Computing and Computer-Assisted Intervention*. Berlin, Heidelberg: Springer, 2000.p557–566. Block matching: A general framework to improve robustness of rigid registration of medical images. In: pp.
- Paulini F, Chaves SB, Rolo JIJ, Azevedo RB, Lucci CM. Evaluation of ovarian structures using computerized microtomography. *An Acad Bras Ciênc* 2017;**89**:2131–2139.
- Pepling ME, Spradling AC. Female mouse germ cells form synchronously dividing cysts. *Development* 1998;**125**:3323–3328.
- Pepling ME, Spradling AC. Mouse ovarian germ cell cysts undergo programmed breakdown to form primordial follicles. *Dev. Biol* 2001;**234**:339–351.
- Prozorowska E, Jackowiak H, Skieresz-Szewczyk K. Morphology and topography of internal reproductive organs in the female cat during prenatal and postnatal development: Scanning electron microscope and three-dimensional reconstruction study. *J. Morphol* 2018;**279**: 1764–1775.
- Rawson SD, Maksimcuka J, Withers PJ, Cartmell SH. X-ray computed tomography in life sciences. *BMC Biol* 2020;**18**:21.
- Regev A, Teichmann SA, Lander ES, Amit I, Benoist C, Birney E, Bodenmiller B, Campbell P, Carninci P, Clevers H, Human Cell Atlas Meeting Participants et al. Science forum: the human cell atlas. *Elife* 2017;**6**:e27041.
- Richardson SJ, Senikas V, Nelson JF. Follicular depletion during the menopausal transition: evidence for accelerated loss and ultimate exhaustion. *J Clin Endocrinol Metab* 1987;**65**:1231–1237.
- Richardson DS, Lichtman JW. Clarifying tissue clearing. *Cell* 2015; **162**:246–257.
- Richardson DS, Lichtman JW. SnapShot: tissue clearing. *Cell* 2017; **171**:496–496.
- Rinaldi VD, Hsieh K, Munroe R, Bolcun-Filas E, Schimenti JC. Pharmacological inhibition of the DNA damage checkpoint prevents radiation-induced oocyte death. *Genetics* 2017;**206**:1823–1828.
- Saalfeld S. Computational methods for stitching, alignment, and artifact correction of serial section data. *Methods Cell Biol* 2019;**152**: 261–276.
- Sahiner B, Pezeshk A, Hadjiiski LM, Wang X, Drukker K, Cha KH, Summers RM, Giger ML. Deep learning in medical imaging and radiation therapy. *Med Phys* 2019;**46**:e1–e36.
- Santi PA. Light sheet fluorescence microscopy: a review. *J Histochem Cytochem* 2011;**59**:129–138.
- Sethian JA. *Level Set Methods and Fast Marching Methods: evolving Interfaces in Computational Geometry, Fluid Mechanics, Computer Vision, and Materials Science*. Cambridge, UK: Cambridge university press, 1999.
- Silva JMDS, Zanette I, Noël PB, Cardoso MB, Kimm MA, Pfeiffer F. Three-dimensional non-destructive soft-tissue visualization with X-ray staining micro-tomography. *Sci Rep* 2015;**5**:1–7.
- Tam PPL, Snow MHL. Proliferation and migration of primordial germ cells during compensatory growth in mouse embryos. *J Embryol Exp Morphol* 1981;**64**:133–147.
- Thet-Thet-Lwin YA, Imai M, Maruyama H, Hyodo K, Takeda T. Testicular seminoma in the aged rat visualized by phase-contrast X-ray computed tomography. *Acta Radiol Open* 2018;**7**: 2058460118806657.
- VanHorn S, Morris SA. Next-Generation Lineage Tracing and Fate Mapping to Interrogate Development. *Dev Cell* 2020; **S1534-5807**:30841–30848.
- Van Reeth E, Tham IW, Tan CH, Poh CL. Super-resolution in magnetic resonance imaging: a review. *Concepts Magn Reson* 2012; **40A**:306–325.
- Wassarman PH. *The Physiology of Reproduction*. New York, USA: Raven press, 1988.The mammalian ovum. In: Eds. E Knobil and JD. Neill
- Zehbe R, Haibel A, Riesemeier H, Gross U, Kirkpatrick CJ, Schubert H, Brochhausen C. Going beyond histology. Synchrotron micro-computed tomography as a methodology for biological tissue characterization: from tissue morphology to individual cells. *J R Soc Interface* 2010;**7**:49–59.